Available online at www.sciencedirect.com
ScienceDirect
Journal of Power Sources 159 (2006) 1115–1122
JOURNAL OF POWER SOURCES
www.elsevier.com/locate/jpowsour

Contact resistance prediction and structure optimization of bipolar plates

P. Zhou, C.W. Wu *, G.J. Ma

National Key Laboratory of Structure Analysis for Industrial Equipment, Department of Engineering Mechanics, Dalian University of Technology, Dalian 116024, China

Received 5 November 2005; received in revised form 17 December 2005; accepted 20 December 2005
Available online 23 February 2006

Abstract

The objective of this work is to investigate the effect of clamping force on the interfacial contact resistance and the porosity of the gas diffusion layer (GDL) in a proton exchange membrane fuel cell (PEMFC). An optimal rib shape for the bipolar plate is developed to analyze the electrical contact resistance. We found that the electrical contact resistance is determined by both the clamping force and the contact pressure distribution. A minimum contact resistance can be obtained in the case of a constant contact pressure distribution. The porosity of the GDLs underneath the rib of the bipolar plate decreases with increasing the clamping force, and the void volume is changed with the deformation of the GDLs. It is found that there exists an optimal rib width of the bipolar plates to obtain a reasonable combination of low interfacial contact resistance and good porosity for the GDL.

Keywords: Fuel cells; PEMFC; Contact resistance; Diffusion layer; Clamping force

1. Introduction

The basic working mechanism of electrochemical fuel cells (FC) is to convert fuel and oxidant directly into electricity energy. Since 1839, when Grove [1] demonstrated a primitive fuel cell, great progress has been made in the research and development of fuel cells. Today, fuel cells are considered to have a great future due to their zero pollution, high efficiency and very low noise. Among the fuel cells under development, the polymer electrolyte membrane fuel cell (PEMFC) is considered as the first candidate for a power source for automobiles because of its low-temperature operation, high power density, fast start-up and system robustness. During the past 20 years, much attention has been placed on the research and development of the PEMFC with a Nafion® membrane as electrolyte. To increase the power density, many researchers have focussed their attention on novel membrane electrolytes, catalysts and structures, as well as on electrode materials (gas diffusion layers) and their preparation. In a single PEMFC, a polymer membrane is inserted between two gas diffusion layers (GDLs) coated with catalyst, which is further sandwiched between two bipolar plates housing the flow channels. In a practical application, multiple fuel cells are stacked together to give a sufficiently high power and desired voltage.

The gas diffusion layer, catalyst and membrane are usually united together as a membrane electrode assembly (MEA) before stack fabrication. During the clamping process of a fuel cell stack, MEAs, bipolar plates, end plates and gaskets are finally clamped together, as shown in Fig. 1. The gas diffusion layers are made of highly porous materials, and thus are deformed very much in the clamping process. The membrane may be also deformed greatly due to its low elastic modulus. The compression and deformation of the MEA depends on many parameters, such as the elastic modulus and thickness of the MEA, clamping force, the pressures of the fuel and oxidant, gasket material and thickness, temperature, humidity, etc. The deformation of those materials affect directly the efficiency of the fuel cell stack [2,3]. If the clamping force is unreasonably small, the interfacial contact resistance between the gas diffusion layer and bipolar plate will be increased and thus the system efficiency is reduced [3–5]. However, if the clamping force is unreasonably large, the efficiency will be also decreased. In

* Corresponding author. Tel.: +86 411 8470 6353; fax: +86 411 8470 8393.
E-mail address: cwwu@dlut.edu.cn (C.W. Wu).

0378-7753/$ – see front matter © 2006 Published by Elsevier B.V.
doi:10.1016/j.jpowsour.2005.12.080

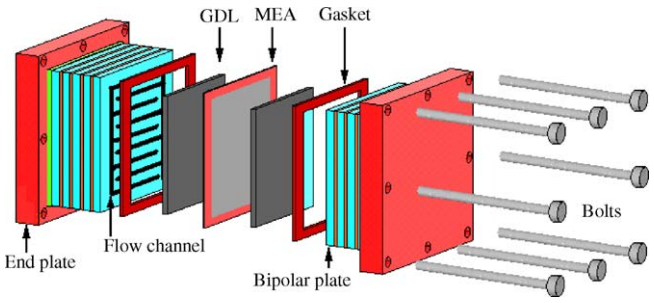

Fig. 1. Schematic of a PEM fuel cell and the locations of the components.

addition, if it is too large, the MEA components may be damaged, causing cell leakage and internal shorts. Experiments have showed that there is an optimum clamping force for a real fuel cell stack [3].

After being clamped together in a fuel cell system, the gas diffusion layer may be one of the components with the most deformation. Thus, the permeability or the pore size may be changed very much. This, in turn, influences greatly the power density or efficiency of the fuel cell system [6–8], especially in an inter-digital flow channel [9] or with serpentine flow channels [8]. In the present paper, we first theoretically study the influence of the clamping force and the width of the rib on the interfacial contact resistance and porosity of the gas diffusion layer, then, we will discuss their possible effects on performance of a fuel cell.

2. Contact resistance model

Multiple fuel cells are stacked together in most practical applications to provide sufficiently high power and voltage. In PEMFCs a gas diffusion layer contacts directly with the bipolar plates. The interfacial electrical contact resistance between them is one of the important factors leading to operational voltage loss, and can significantly affect the performance of a fuel cell system [10]. The contact resistance of a pair of solid surfaces is governed by the multi-scale surface topography (roughness) and the surface chemical property (a thin layer of oxide or contamination). When two solid surfaces contact each other with a very small compression force, only the tips of the roughness come into real contact and thus the real contact area is very small [11,12]. It was found that the contact resistance decreased non-linearly with compression force.

Several groups of experimental data on the interfacial contact resistance of a single fuel cell or the total resistance that includes the bulk resistance are available in the literature [5,13,14]. In a fuel cell, the contact resistance may totally differ from that of elastic solids since the GDL is a layer of composite-porous material. Mishra et al. [13] measured the total resistance and the interfacial contact resistance between different gas diffusion layers and graphite bipolar plates. A fractal asperity-based model was adopted to predict the interfacial contact resistance as a function of pressure, material properties and surface geometry. Wang et al. [5] reported the interfacial contact resistances between a Toray carbon paper (Electro-Chem Inc.) and four types of stainless steel bipolar plates. A stainless steel bipolar plate is considered to be one of the best candidates for bipolar plates due to its low cost, high strength, ease of machining and shaping into thin sheets, as well as its high corrosion resistance [5]. Ihonen et al. [14] conducted in situ measurements of the interfacial contact resistance as a function of time, clamping pressure, gas pressure and current density. All the experimental studies mentioned above are focused on the effects of clamping pressure on the interfacial contact resistance. It was found that the interfacial contact resistance decreases quickly with the clamping force at a small clamping force, and reaches almost a saturation level at high clamping force.

There are many researches on the electricity/heat conduction of two contact surfaces [11,12,15], giving a few topography-based theoretical models. The mechanisms of electricity and heat conduction are similar to each other, strongly depending on the real contact area. However, the topography parameters used in the model are very complex and difficult to measure. In addition, no research work was found to consider such a special structure of random fibre network as a carbon paper. Different fabrications of the GDLs and bipolar plates produce different interfacial contact resistances. In the present work, we use an equation based on the work of Mishra et al. [13] to calculate the total interfacial contact resistance. Generally speaking, the relationship between interfacial resistance and contact pressure can be expressed by following equation:

$$R = \frac{1}{A_a} A \left(\frac{B}{p} \right)^C \tag{1}$$

where A_a is the apparent contact area of the interface, p the contact pressure and A, B and C are parameters determined by experiments. According to Eq. (1), we can get the interfacial contact resistivity:

$$\rho = A \left(\frac{B}{p} \right)^C \tag{2}$$

We found that the interfacial contact resistivity measured by Mishra et al. [13] and Wang et al. [5] can be fitted by Eq. (2) with a pretty good accuracy, as shown in Fig. 2. The values of fitted parameters are shown in Table 1. A high contact pressure can decrease the total electrical contact resistance. On the other hand, the clamping force can change the porosity of gas diffusion layer. A higher porosity may be expected to decrease the mass transfer resistance of a gas phase, especially in a PEM fuel cell with inter-digital flow field as shown in Fig. 3.

Gas diffusion layer does much more than diffusing the gas and forming an electrical connection between the catalyst layer and the bipolar plate. In addition, it carries water, an important reaction product, away from the electrolyte surface, and also forms a protective layer over the very thin layer of the catalyst. When a fuel cell system is stacked, the void volume in gas diffusion layer underneath the rib will decrease with the clamping force. For each fuel cell system, there might be an optimal choice of the clamping force.

Table 1
Parameters of the interfacial contact resistance function for gas diffusion layers and the bipolar plate

Bipolar plate	GDL	A (mΩ cm^2)	B (MPa)	C	Reference
Graphite	GDL-10BA	3.32	1.01	0.534	Mishra et al. [13]
Graphite	GDL-10BB	3.72	0.966	0.692	Mishra et al. [13]
Stainless steel	Carbon paper	81.4	2.52	1.07	Wang et al. [5]

GDL-10BA and GDL-10BB are two kinds of paper-based GDL (SGL Carbon Group).

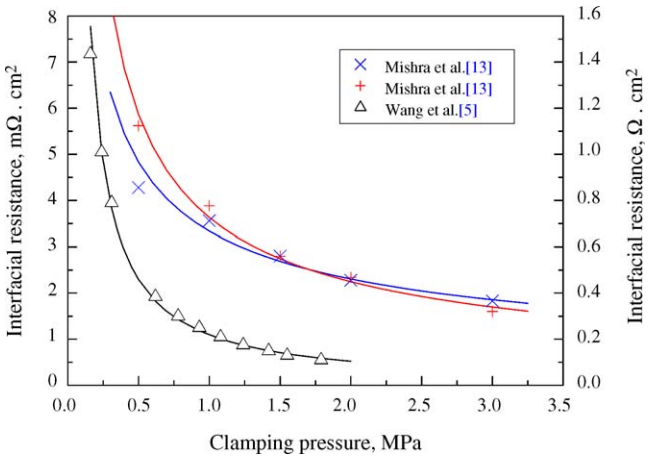

Fig. 2. Variation of the interfacial contact resistance over a range of clamping pressures.

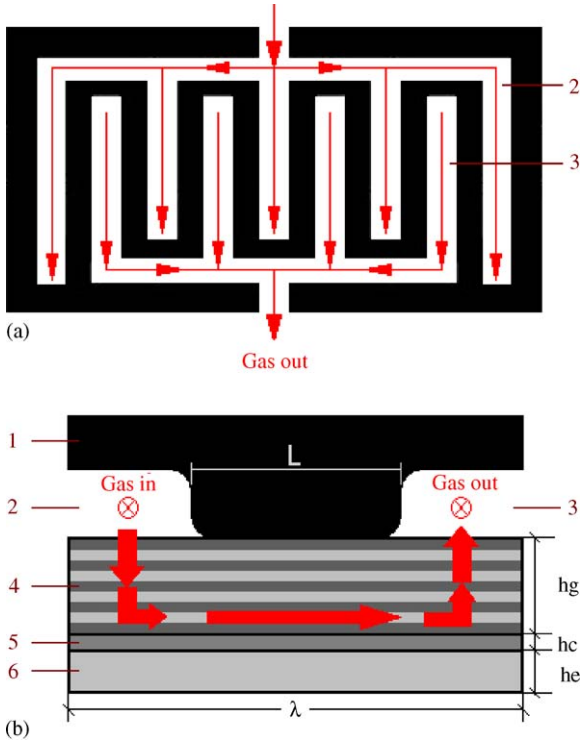

Fig. 3. (a) Schematic of an inter-digital flow field and (b) a typical cross-section. 1, Bipolar plate (current collector); 2, inlet gas channel; 3, outlet gas channel; 4, gas diffusion layer; 5, catalyst layer and 6, membrane.

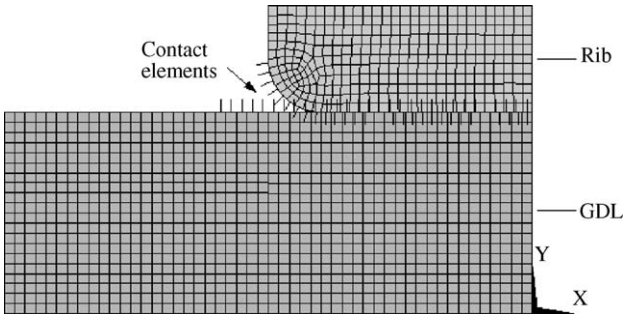

Fig. 4. FEM model of a bipolar plate rib contacting with a GDL.

3. Analysis method

3.1. Finite element meshes and material parameters

We used the finite element method (FEM) to analyze the contact pressure and the bulk strain of the gas diffusion layer. The FEM analysis model is shown in Fig. 4. In order to save computation time, the computational domain consists of half a period of the flow channel and rib, i.e., the left half of the area of Fig. 3b. It is assumed that the structures of the cathode and anode of the bipolar plates have the same shape, and the compressive modulus of catalyst layer and membrane are much higher than that of the gas diffusion layer. The round radius of the rib will change the local pressure distribution, and it is very important to avoid stress concentration leading to possible damage of the local strctural materials. The normal displacements at the left, right and bottom boundaries of the gas diffusion layer were restricted due to the symmetry of the structure. The vertical displacement of the rib is given downwards, simulating the stacking process.

The problem mentioned above can be described as a large deformation contact problem with plane-strain and free boundary. The meshes of finite elements were designed as shown in Fig. 4. Plane-strain elements with eight nodes were used and contact elements were built in the contact region. Table 2 shows

Table 2
Compression modulus as a function of pressure for GDLs[13]

GDL	Pressure range (MPa)	E (MPa)
GDL-10BA	0.00–0.15	1.71
	0.15–1.12	4.59
	0.12–3.00	6.16
GDL-10BB	0.00–0.16	1.81
	0.16–0.52	5.11
	0.52–3.00	8.57

the compressive modulus of the gas diffusion layers as a function of the relevant pressure range [13]. It was observed that the GDLs have three regions of linear elasticity. The GDL is a layer of anisotropic porous material. The elastic modulus in x direction (in-plane direction) is different from that in y direction (normal direction). However, due to the symmetry of the fuel cell structure and the very thin GDL layer compared to the other dimensions, the in-plane deformation was constrained in the numerical analysis. In fact the in-plane deformation has relatively insignificant effects on the contact pressure and bulk strain. Consequently, the in-plane mechanical properties are not important to the parameters studied in the present paper, and we assume that the GDL is isotropic. In order to check the validity of the assumption, we used the in-plane elastic modulus ranging from 5 to 50 MPa, and found that this gave rise to a change of the contact pressure and bulk strain less than 1.5%.

3.2. Interfacial contact resistance

The interfacial contact resistance between two surfaces is considered as an electric circuit in a parallel connection, as shown in Fig. 5, supposing that the surface is equipotential. The interfacial contact resistance can be calculated using the equation given in Fig. 5 with the continuous distribution of interfacial contact resistance, where ρ is the electrical resistivity, R_B the bulk resistance of bipolar plate, R_G the bulk resistance of gas diffusion layer and $R_{G/B}$ is the contact resistance between gas diffusion and bipolar plate. After the numerical solution of the interfacial contact pressure, we can get the discrete contact pressure distribution. The total interfacial contact resistance can be calculated using the following equation:

$$R = \frac{1}{\sum_{i=1}^{n} \frac{1}{R_i}} = \frac{1}{\sum_{i=1}^{n} \frac{S_i}{A(B/p_n^i)^C}} \tag{3}$$

where S_i and n denote the boundary area of the ith contact element and the number of contact elements, respectively. The total compression force, F, has the following relationship with the contact stress components:

$$\vec{F} = \sum_{i=1}^{n} p_n^i \vec{n} + p_\tau^i \vec{\tau} \tag{4}$$

where p_n^i is the normal contact stress component (contact pressure), p_τ^i the tangential contact stress component, $\vec{n}$ and $\vec{\tau}$ are the unit vectors in normal and tangential directions, respectively.

3.3. Porosity of the GDL

The GDL is a porous elastic material. The porosity of porous media is defined as:

$$\varphi = \frac{V_p}{V} \tag{5}$$

where V_p is the void volume and V is the total volume of porous media. Based on the definition of porosity, we can get the porosity of GDL after stacking:

$$\bar{\varphi} = \frac{\bar{V}_p}{\bar{V}} = \frac{V_0\varphi_0 - V_0\varepsilon_v}{V_0(1-\varepsilon_v)} = \frac{\varphi_0 - \varepsilon_v}{1-\varepsilon_v} \tag{6}$$

where V_0 is the initial total volume of porous media, φ_0 the initial porosity and ε_v is the bulk strain ($\varepsilon_v = \varepsilon_x + \varepsilon_y + \varepsilon_z$). The top-bar means the variables after stacking. We also defined a relative porosity for comparison with the initial void volume:

$$\tilde{\varphi} = \frac{\bar{V}_p}{V_0} = \frac{V_0\varphi_0 - V_0\varepsilon_v}{V_0} = \varphi_0 - \varepsilon_v \tag{7}$$

Eqs. (6) and (7) are based on the small deformation assumption, and the error is about 5.7% when the bulk strain is within 0.3. Obviously, the porosity of a gas diffusion layer after stacking loading is not uniform any more. The minimum porosity of

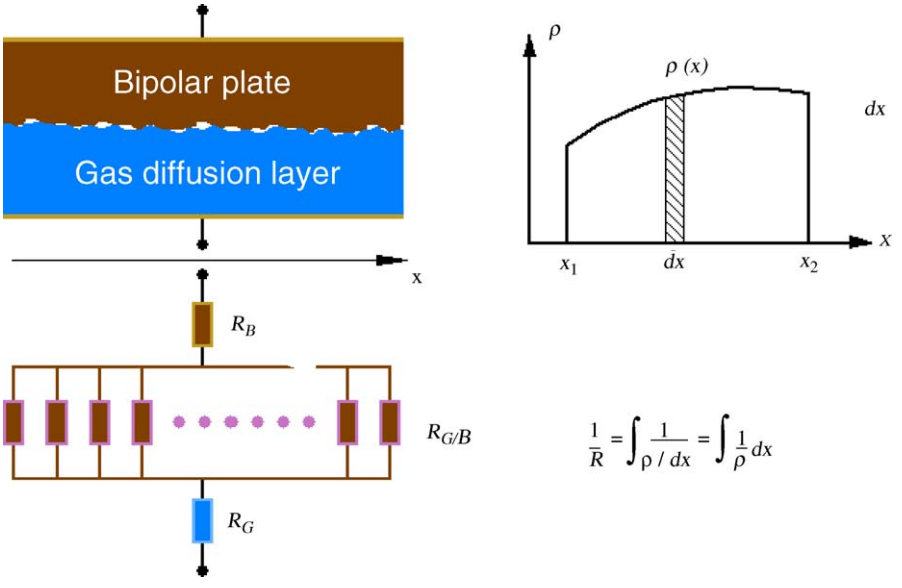

Fig. 5. Schematic of the contact electrical circuit in a parallel connection.

gas diffusion layer occurs underneath the middle of rib ($x = 0$ in Fig. 4), where the GDL gives a largest deformation.

4. Numerical results and analysis

4.1. Optimization of the contact pressure distribution

From Eq. (3), the total interfacial contact resistance for different contact pressure distributions may be totally different, even with the same clamping force. Distributions of the contact pressures are determined by the mechanical and geometrical properties of the bipolar plates. An optimum rib shape producing a minimum interfacial contact resistance is expected in fuel cell stack design. However, it is difficult to exactly optimize the rib shape directly. The first question is what a contact pressure distribution gives a minimum contact resistance when the total compression force is fixed. The optimum problem can be described as follows:

$$\begin{aligned} &\text{find} && p_n(x) \\ &\min. && R = R(p_n) \\ &\text{s.t.} && \int_0^l p_n \, \mathrm{d}x = F \end{aligned} \tag{8}$$

The design variable is the contact pressure distribution, and the objective function, i.e., contact resistance, is a function of contact pressure distribution. In the present paper, the optimum contact pressure was first obtained, and then the optimum rib shape, which gives an optimum contact pressure distribution, was chosen. The optimization process shows that a constant pressure distribution is an optimum pressure distribution:

$$p(x) = \frac{F}{L} \tag{9}$$

where L is the length of contact region. The second question is what a rib shape of the bipolar plate gives a constant pressure distribution. The pressure distribution is almost a constant value when the cross-shape of rib is rectangular. When the GDL is loaded with a constant distributed pressure, an optimum rib shape can be found approximately from the deformation of the GDL surface (see Fig. 6a), similar to a rectangular rib with round corner. However, the optimum rib may be more difficult for machining than a traditional rectangular rib.

The contact pressure approaches to infinity if the corner of rectangle rib is a right angle, and an increase of the round radius reduces the local pressure. We should design a reasonable round radius to reduce the local stress concentration. However, too big

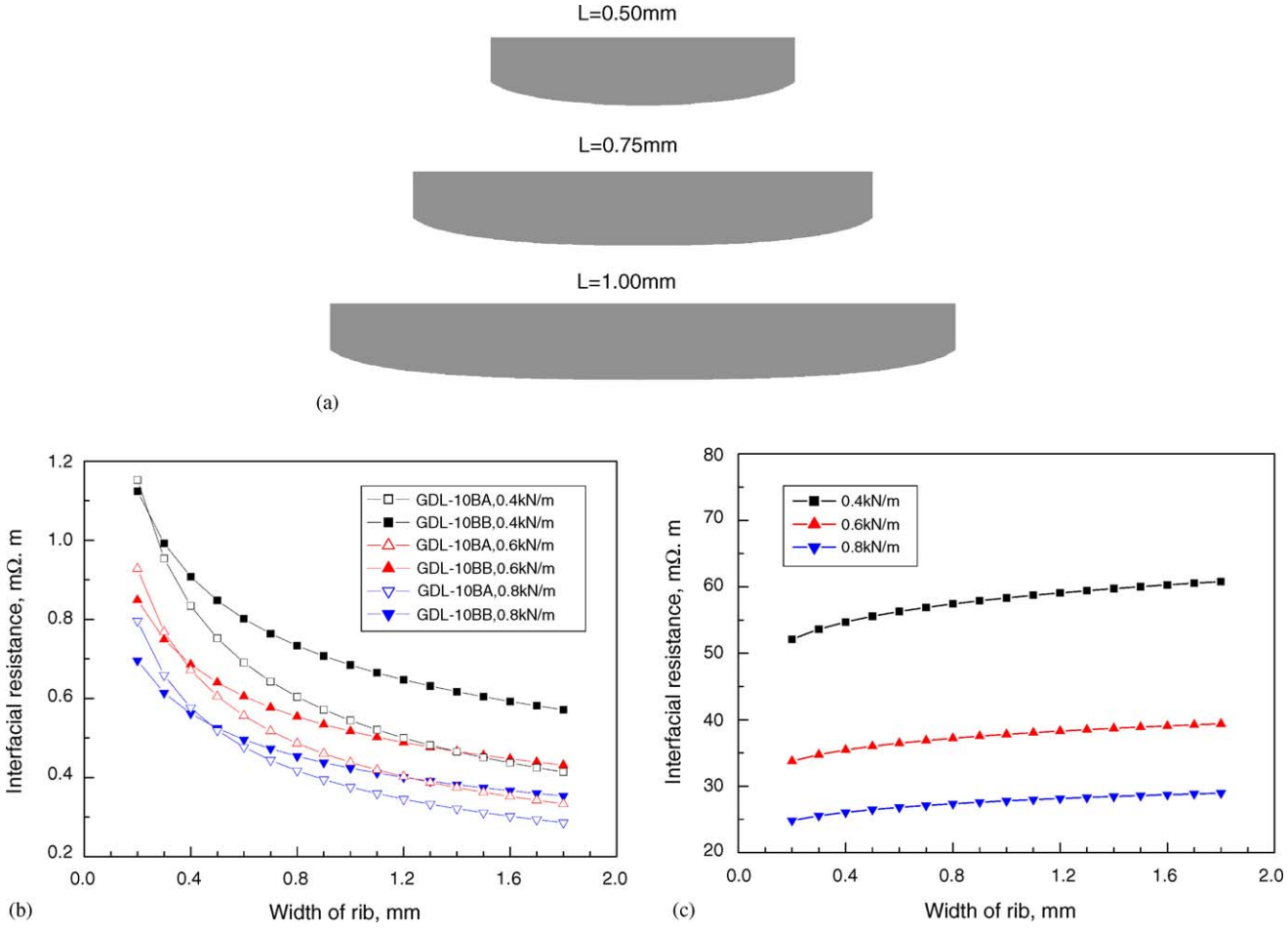

Fig. 6. (a) Optimum rib shape with different widths of rib when $\lambda = 2$ mm, $h_g = 0.5$ mm and the contact pressure is 1 MPa; (b) interfacial contact resistance at various rib widths and clamping forces for graphite bipolar plate and (c) interfacial contact resistance at various rib widths and clamping forces for stainless steel bipolar plate.

a round radius will increase the contact resistance. The reason is shown later from the comparison of the contact resistances produced by a rectangular rib and a semicircular rib. In this study, the round radius is 0.04 mm.

4.2. Effects of rib length and clamping force on the interfacial contact resistance

Using the experiential formula (3), one obtains:

$$R = \frac{A}{L}\left(B\frac{L}{F}\right)^{C} = A\left(\frac{B}{F}\right)^{C} L^{C-1} \tag{10}$$

From Eq. (10), one obtains:

$$\frac{\partial R}{\partial L} = A\left(\frac{B}{F}\right)^{C} L^{C-2}(C-1) \tag{11}$$

The experimental observations [13] show that C is a constant less than 1 for a graphite bipolar plate. Therefore, the interfacial contact resistance decreases with increasing the rib width. However, it is greater than 1 for stainless steel. The interfacial contact resistance was calculated at various rib widths, as shown in Fig. 6b. It is observed that the interfacial contact resistance decreases rapidly at a small rib width and then decreases gradually at a large rib width, and the resistance of GDL-10BA with lower hardness decreases more quickly than GDL-10BB. When the rib width is fixed, the interfacial contact resistance is sensitive to the clamping force, especially at a value smaller than 0.6 kN m^{-1}. For a stainless bipolar plate, C is greater than 1, as a result the value of Eq. (11) is positive, and the interfacial contact resistance increases with increasing rib width (see Fig. 6c). They are 52.1 and 60.8 mΩ m at the rib width of 0.2 and 1.8 mm ($\lambda = 2$ mm), respectively, when the clamping force is 0.4 kN m^{-1}.

4.3. Porosity distribution in the GDL

Now we will discuss the effect of clamping force on the interfacial contact resistance. On the one hand, a higher clamping force and larger rib width are helpful to reduce the total interfacial contact resistance for a graphite bipolar plate. On the other hand, a higher clamping force results in a decrease of porosity (i.e., the void volume in gas diffusion layer) and an increase of the gas transport resistance. At the same time, electrode flooding may occur. The porosity is a function of the rib width and clamping force (Fig. 7). It is observed that the relative porosity, defined in Eq. (7), decreases much faster than the porosity with a clamping force. This indicates that the deformation of the GDL and clamping force have to be considered when we analyze the gas transport.

Most of the studies in the development of a theoretical model for PEM fuel cells have used for simplicity the assumption of constant porosity in the GDL [16–18]. But Roshandel et al. [19] assumed a variation of porosity across the GDL as:

$$\varepsilon^{\text{comp}}(x) = \varepsilon^{0}\left(\sum_{n} A_n \sin^{2n} x\right) \tag{12}$$

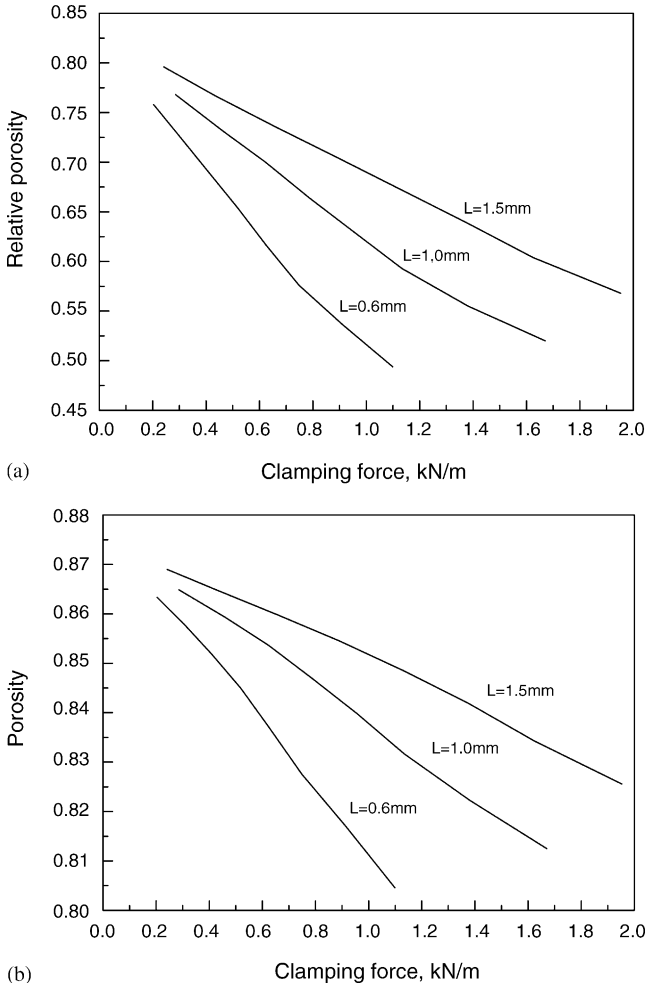

Fig. 7. Porosity (a) and relative porosity (b) decrease as a function of clamping force and rib width.

where ε^{0} is the initial porosity and $\varepsilon^{\text{comp}}$ is the porosity of the GDL after stacking. These models, however, cannot reflect the importance of the void volume change caused by a clamping force.

4.4. Comparison of different GDLs and rib shapes

Two kinds of gas diffusion layers (GDL-10BA and GDL-10BB) with different initial porosity and compressive modulus are studied. Effects of clamping force on contact resistance and relative porosity are shown in Fig. 8 (the width of rib is 1 mm). It is observed that there is an intersection of the two relative porosity curves. At the lower clamping force area, the GDL-10BA with smaller contact resistance and larger relative porosity gives rise to a better performance than GDL-10BB. For the higher clamping force area, however, the contact resistances are almost the same for both of the GDLs, but the relative porosity of the GDL-10BB is larger than that of the GDL-10BA. Thus, the GDL-10BB may give rise to a better performance than GDL-10BA.

Based on the foregoing discussion, we find that the clamping force affects the interfacial contact resistance and the porosity

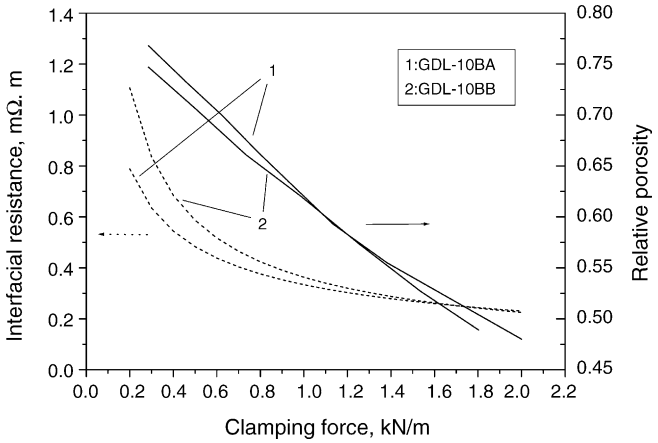

Fig. 8. Effects of clamping force on contact resistance and relative porosity.

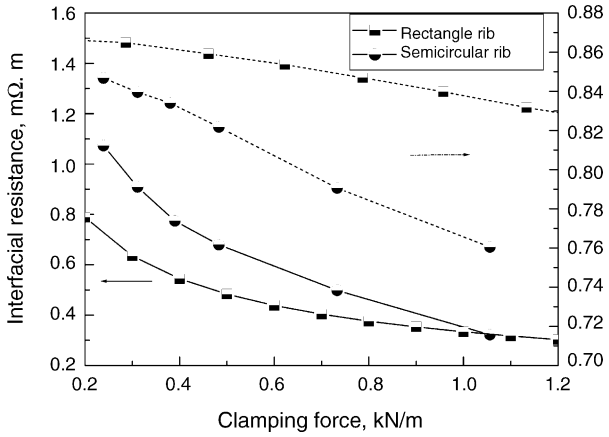

Fig. 10. Effect of rib shape on contact resistance and porosity.

in two opposite ways. A high clamping force can give a low interfacial contact resistance as expected, but also gives rise to a low porosity of GDL, which may decrease the system efficiency. The shape of the rib is one of the important factors affecting the contact pressure distribution, contact resistance and the porosity of GDL. We now study the effects of rib shape (rectangular and semicircular) on the contact resistance and porosity of GDLs. Fig. 9 shows distribution of the porosity with the same clamping force but different shapes of rib cross-sections. It is observed that the porosity of the GDL contacting with the semicircular rib is smaller than that when contacting with a rectangular rib.

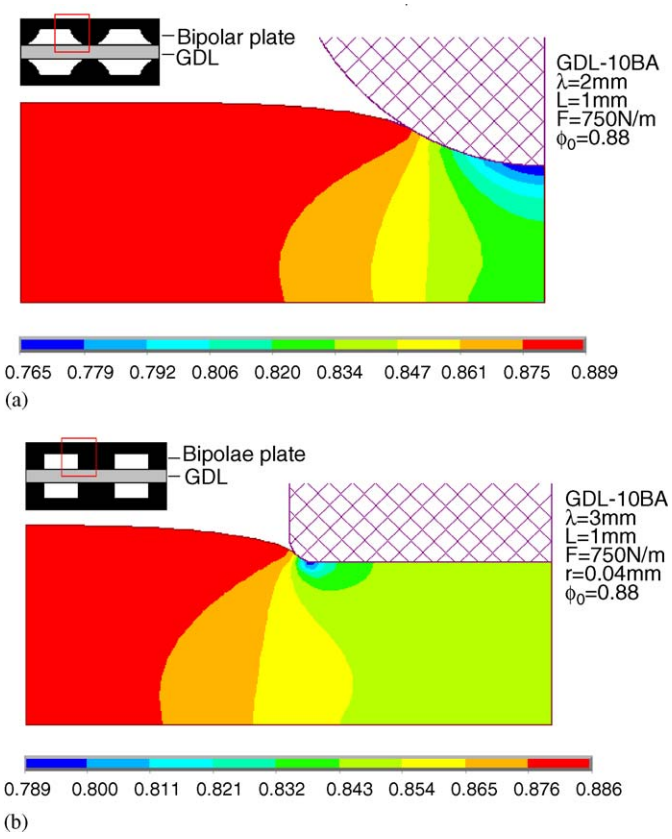

Fig. 9. The porosity distribution in the GDL for different cross-sections of rib: (a) semicircular and (b) rectangular with a round corner.

The permeability, which is related to the porosity, controls the fuel flow distribution in fuel cells. The fuel flow distribution has an important influence on the power density [20–22]. As can be seen from Fig. 10, the rib with a semicircular cross-section results in a higher contact resistance and lower porosity than the rib with rectangle cross-section. When the clamping force per unit length ranges from 0.2 to ~1.0 kN m^{-1}, the rectangular rib is better than the semicircular rib.

5. Discussions

Based on the analysis mentioned above, it is observed that the geometric parameters of bipolar plate, the rib shape, the physical properties of GDL and bipolar plate, and the clamping force will influence the electric resistance and the porosity in GDLs. Experiments of Hentall et al. [23] and Lee et al. [10] indicated that changes in electric resistance and the porosity in the GDL affect the power density of a fuel cell system. In fact, there are more complex parameters, such as the fuel pressure inside the fuel cell, temperature, humidity, thickness of gasket, working together to affect the resistance and porosity. What's more, all the parameters may influence to each other.

In the present paper, the compression force between a GDL and a bipolar plate is found to be one of the key factors to affect the electric resistance and porosity of the GDL. We should notice that in a real PEMFC system the fuel pressure supplied, mechanical and geometrical properties of the gaskets and the contact pressure between GDLs and bipolar plates work together to determine the total clamping force, as shown in Fig. 11. There are several questions which should be paid more attention. The volume of the channel is changed more than 10% due to the deformation of the GDL when the nominal clamping pressure (total clamping force divided by the area of GDL) is about 0.4 MPa. The effect of change in the channel volume on the power density of the fuel cell system should be considered according to the work of Kumar and Reddy [24]. Therefore, the effect of the clamping force on the power density may be deduced from the change in channel volume besides the electric resistance and porosity. On the other hand, the total clamping force is affected by many parameters, such as the inner gas pres-

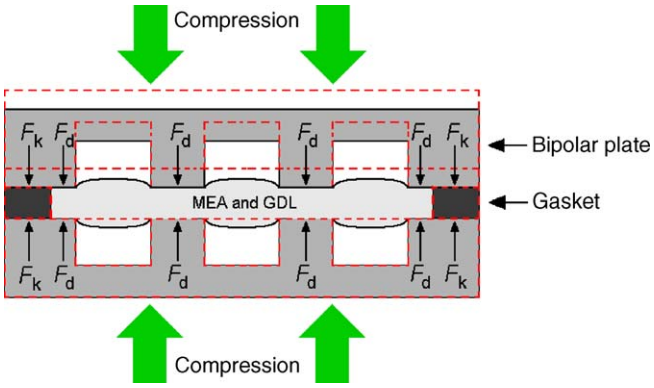

Fig. 11. Schematic of material deformation due to clamping. The dash line represents the structure before stacking.

sure of fuel flow, the force acting on the GDL, and the force acting on the gasket. The contact pressure cannot be obtained though the real clamping force unless using the measurement method of Lee et al. [10]. Another problem is the heat and water produced in the system, which influences the stress distribution due to the different expansibilities of each component. Further work will include these factors using the simulated contact resistance and prediction of polarization curves of the PEM fuel cell system.

In summary, the contributions of the present work are: (1) a contact resistance model was developed; (2) an optimal method together with FEM algorithm was proposed; (3) an optimization design for the rib shape of bipolar plate was given, i.e., a rectangular cross-section with a suitable round radius may be the optimal shape, giving a nearly uniform distribution of contact pressure and a minimum contact resistance and (4) a porosity field for the GDL of a fuel cell was developed together with the stress and strain field.

6. Conclusions

The effect of the clamping force on the interfacial contact resistance and the porosity of the gas diffusion layer was analyzed using the finite element method and a contact resistance model was developed. Numerical results for different rib widths and clamping forces show that a larger clamping force and wider rib lead to a smaller contact resistance when the bipolar plate is made of graphite. However, the porosity of the gas diffusion layer will decrease with increasing clamping force, especially with a semicircular rib. For a stainless bipolar plate there seems to be an optimal rib width to give a reasonable low contact resistance and a high porosity.

The constant pressure distribution is an optimum distribution for getting minimum interfacial electric resistance. This is a preparatory work to optimize the fuel cell system. The results of present study can be used in a comprehensive model of a PEM fuel cell to account for the effect of clamping force on fuel cell performance.

References

[1] W.R. Grove, Philos. Mag. 314 (1839) 127–130.
[2] G.G. Scherer, Solid State Ionics 94 (1997) 249–257.
[3] W.K. Lee, C.H. Ho, J.W.V. Zee, M. Murthy, J. Power Sources 84 (1999) 45–51.
[4] V. Mishra, F. Yang, R. Pitchumani, ASME J. Fuel Cell Sci. Technol. 1 (2004) 2–9.
[5] H. Wang, M.A. Sweikart, J.A. Turner, J. Power Sources 115 (2003) 243–251.
[6] J. Soler, E. Hontanon, L. Daza, J. Power Sources 118 (2003) 172–178.
[7] M. Prasanna, H.Y. Ha, E.A. Cho, et al., J. Power Sources 131 (2004) 147–154.
[8] J.G. Pharoah, J. Power Sources 144 (2005) 77–82.
[9] H. Dohle, R. Jung, N. Kimiaie, et al., J. Power Sources 124 (2003) 371–384.
[10] W. Lee, C. Ho, J.W. Van Zee, et al., J. Power Sources 84 (1999) 45–51.
[11] J.A. Greenwood, J.B.P. Williamson, Proc. R. Soc. A295 (1966) 300–319.
[12] J.B.P. Williamson, Proceedings of the 4th International Conference On Electrical Contact Phenomena, Swansea, 1968, pp. 30–34.
[13] V. Mishra, F. Yang, R. Pitchumani, ASME J. Fuel Cell Sci. Technol. 1 (2004) 2–9.
[14] J. Ihonen, F. Jaouen, et al., Electrochim. Acta 46 (2001) 2899–2911.
[15] A. Majumdar, C.L. Tien, Trans. ASME 113 (1991) 516–525.
[16] D. Singh, D.M. Lu, N. Djilali, Int. J. Eng. Sci. 37 (1999) 431–452.
[17] A. Rowe, X. Li, J. Power Sources 102 (2001) 82–96.
[18] J.S. Yi, T.V. Nguyen, J. Electrochem Soc. 146 (1999) 38–45.
[19] R. Roshandel, B. Farhanich, E. Saievar-Iranizad, Renewable Energy 30 (2005) 1557–1572.
[20] H. Dohle, R. Jung, N. Kimiaie, J. Mergel, M. Muller, J. Power Sources 124 (2003) 371–384.
[21] J. Soler, E. Hontanon, L. Daza, J. Power Sources 118 (2003) 172–178.
[22] M. Prasanna, H.Y. Ha, E.A. Cho, S.A. Hong, I.H. Oh, J. Power Sources 131 (2004) 147–154.
[23] P.L. Hentall, J.B. Lakeman, G.O. Mepsted, P.L. Adcock, J. Power Sources 80 (1999) 235–241.
[24] A. Kumar, R.G. Reddy, J. Power Sources 131 (2003) 11–18.